Published in final edited form as:

Anal Chem. 2020 November 03; 92(21): 14558–14567. doi:10.1021/acs.analchem.0c02799.

Electroosmotic Perfusion–Microdialysis Probe Created by Direct Laser Writing for Quantitative Assessment of Leucine Enkephalin Hydrolysis by Insulin-Regulated Aminopeptidase in Vivo

Rachael E. Wilson,
Department of Chemistry, University of Pittsburgh, Pittsburgh, Pennsylvania 15260, United States;

Andrea Jaquins-Gerstl,
Department of Chemistry, University of Pittsburgh, Pittsburgh, Pennsylvania 15260, United States;

Jun Chen,
Department of Electrical and Computer Engineering, and Petersen Institute of NanoScience and Engineering, University of Pittsburgh, Pittsburgh, Pennsylvania 15260, United States;

Michael Rerick,
Department of Chemistry, University of Pittsburgh, Pittsburgh, Pennsylvania 15260, United States;

Stephen G. Weber
Department of Chemistry, University of Pittsburgh, Pittsburgh, Pennsylvania 15260, United States;

Abstract

There are many processes that actively alter the concentrations of solutes in the extracellular space. Enzymatic reactions, either by soluble enzymes or membrane-bound ectoenzymes, and uptake or clearance are two such processes. Investigations of ectoenzymatic reactions in vivo is challenging, particularly in the brain. Studies using microdialysis have revealed some qualitative information about what enzymes may be present, but microdialysis is a sampling technique so it is not designed to control conditions such as a substrate concentration outside the probe. Micropush–pull perfusion has been used to determine which nitric oxide synthase enzymes are

Corresponding Author: Stephen G. Weber – *Department of Chemistry, University of Pittsburgh, Pittsburgh, Pennsylvania 15260, United States;* sweber@pitt.edu.

Supporting Information

The Supporting Information is available free of charge at https://pubs.acs.org/doi/10.1021/acs.analchem.0c02799.
Figures: S1: LC-MS2 calibration curve; S2 and S3: Images of the EOP-MD probe; S4: Fluorescence measurements of in vitro EOP; S5: Probe placements. Sections: S1 Semiquantitative explanation of the effect of current on the collection efficiency of the (unreactive) internal standard (Figure 5). S2 Experimental Methods: S2.1 Construction of current source/sink and EOF generation S2.2 Synthesis of hydrogels and fluorescence imaging S2.3 Fluorescence measurements S2.4 LC-MS^2 S2.5 Animal surgeries (PDF)

Complete contact information is available at: https://pubs.acs.org/10.1021/acs.analchem.0c02799

Notes

The authors declare no competing financial interest.

active in discrete regions of the rat retina. Ectopeptidases are a particularly important class of ectoenzymes. As far as it is known, the extracellular activity of active peptides in the brain is controlled by ectopeptidases. To understand ectopeptidase activity, we developed a physical probe and an accompanying method. The probe has a two-channel source that supplies substrate or substrate plus inhibitor using electroosmotic perfusion (EOP). It also has a microdialysis probe to collect products and unreacted substrate. The method provides quantitative estimates of substrate-to-product conversion and the influence of inhibitors on this process. The quantitative estimates are made possible by including a D-amino acid-containing peptide analog of the substrate in the substrate-containing solution infused. Quantitative analysis of substrate, substrate analog, and products is carried out by quantitative, online capillary liquid chromatography-tandem mass spectrometry. The electroosmotic perfusion-microdialysis probe and associated method were used to determine the effect of the selective inhibitor HFI-419 on insulin-regulated aminopeptidase (EC 3.4.11.3) in the rat neocortex.

Graphical Abstract

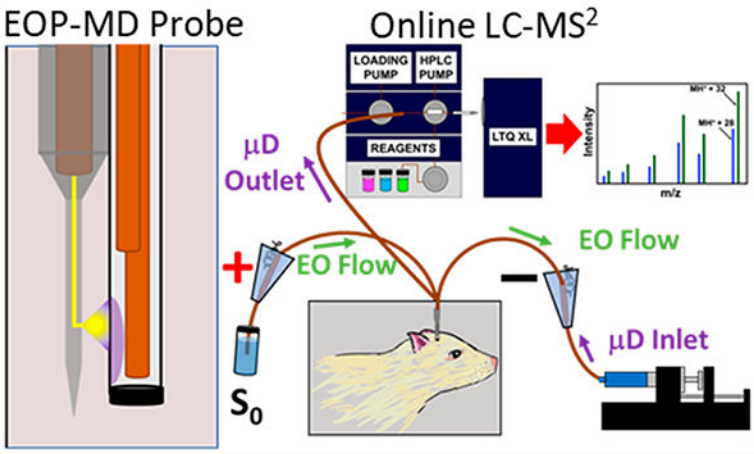

Ectopeptidases, membrane-bound enzymes with active sites facing the extracellular space,[1] modulate the effects of neuropeptides[2] in the brain. Hydrolysis products can have effects that are different from the parent peptide.[3] Thus, ectopeptidases control the local activity of neuropeptides. The understanding of such processes quantitatively is limited by the lack of suitable methods.[4] Quantitative measurements of ectopeptidase activity are especially challenging in the brain where the role of a peptidase can be tied to its specific location,[1,2] requiring spatially resolved methods for probing the extracellular space. In vitro assays[5–8] and in situ histological studies using zymography and MALDI mass spectrometry[9–13] provide important information, but it is unknown how activities implied by these methods translate to in vivo conditions.[14,15] There exists a need for a sampling-based method for assessing membrane-bound ectopeptidase activity using natural substrates in an in vivo model, particularly in the brain.

Microdialysis[16](MD) has been used to study enzyme activity qualitatively in vitro[8,17] and in vivo in the brain[18–27] and other tissues.[28–34] Substrate introduction through the membrane (retrodialysis or reverse microdialysis) and collection of substrate and products

depends on diffusion, probe characteristics and chemical processes in the tissue.[35–38] In this measurement, the substrate residence time in the tissue cannot be controlled.[39] Reed et al.[23,26] used a commercial probe with a central infusion line to pump peptide substrate into the brain and determine what fragments of substrate peptide were produced. This method is an improvement over using passive diffusion through the microdialysis membrane to introduce peptide substrate because the amount and concentration of peptide introduced are known, for example, 2 μL of 1 mM β-endorphin in rat striatum.[26] In work outside the brain, the Stenken group has explored using the extraction fraction, the ratio of the concentration of substrate collected at the probe outlet compared to that introduced at the inlet, as a measure of enzymatic activity.[8,17,31,32,39,40] They concluded that because the extraction fraction is more affected by mass transport processes than hydrolysis in tissue, it cannot be used to give quantitative information.[39] The major advantage of microdialysis is that it is specific to a particular brain region, and that the measurements are in functioning tissue. There are disadvantages to the microdialysis measurements cited. One is that there is no control over the substrate/product peptide distribution outside of the probe. The peptides move chiefly by diffusion augmented, in the case of Reed et al. by fluid flow that is likely to be along the outside of the probe as noted by researchers attempting drug infusion into the brain by “convection enhanced delivery”.[41] Collection of the products is less efficient the farther from the probe the hydrolysis takes place, so the measurements end up being very sensitive to the environment immediately adjacent to the dialysis membrane.

Iontophoresis has been used sparingly for analogous work. Qualitative evaluation of peptide hydrolysis in skin following iontophoretic delivery has been investigated for Tyr-Phe,[42] LHRH,[43] and delta sleep-inducing peptide.[44] Felix and Harding used iontophoresis to identify the role of enzymatic hydrolysis of angiotensin(III) on its activity.[45] Low-flow push–pull perfusion has been used to identify different nitric oxide synthase subtypes in rat retina based on measuring nitrate concentration in the presence and absence of specific inhibitors.[46] These methods provide a way to determine what enzymes are present in tissue. What is needed is a method to provide more quantitative information specifically about ectopeptidase activity, such as the fraction of introduced substrate that is hydrolyzed in a certain time and how that depends on the concentration of an inhibitor.

Brain tissue supports electroosmosis.[47–50] Thus, we developed a method to determine ectopeptidase activity in organotypic hippocampal slice cultures (OHSCs) using electroosmotic flow.[51–56] The physical arrangement had a pulled capillary as a source of substrate inserted into the tissue and a capillary perpendicular to the culture’s top surface to collect products and unreacted substrate.[57] Electroosmotic flow has several advantages. Importantly, the substrate residence time in the tissue can be controlled by changing the current. A practical advantage is that there is little or no lag time to establish steady-state flow upon changing current.[51,52,55,57] Electroosmotic push–pull perfusion (EOPPP) has been used to identify differential hydrolysis rates of galanin[52] and leucine enkephalin[56] (LE) separately in the CA1 and CA3 regions of OHSCs. Using EOPPP, we found that the activity of a bestatin-sensitive ectopeptidase was higher in CA1 than CA3.[56] This explains CA1’s greater sensitivity to oxygen-glucose deprivation. It unfortunately inactivates the neuroprotective LE, which acts at the δ-opioid receptor, more effectively than the CA3.

EOPPP represents a major technological step in quantitative evaluation of ectopeptidase activity in intact tissue using natural substrates. However, it is obviously preferable to perform these measurements in vivo. Transitioning to in vivo models is not straightforward. There are several requirements for a device that would be able to infer ectopeptidase activity in vivo. One is that it must be capable of quantitative control over the time that peptide is exposed to enzyme. Another is that it should permit matched pairs of experiments, for example, peptide versus peptide plus inhibitor. Finally, the measurement should be designed to minimize the hydrolysis of peptide substrates after the peptide substrate leaves the brain to be measured.

Direct laser writing has been used in the development of tools for working with living systems.[58–75] Notably, the Venton group developed carbon microelectrodes with advantageous properties by using direct laser writing followed by pyrolysis.[76] Using this process (Nanoscribe), we have fabricated a dual-channel electroosmotic perfusion–microdialysis (EOP-MD) probe that allows infusion of a natural substrate from a source into the extracellular space where it interacts with ectopeptidases. Hydrolysis products along with any unhydrolyzed substrate are collected using the integrated MD probe. Dialysate is analyzed online using high-performance capillary liquid chromatography-tandem mass spectrometry (cLC-MS^2). This allows the monitoring of ectopeptidase activity in near-real time with a spatial resolution of approximately 100 μm. Because substrate perfusion velocity is dictated by current, we can control the substrate residence time in the ECS of the tissue by changing the magnitude of the current.[55,56] The dual-channel perfusion tip permits sampling under a pair of matched conditions (±inhibitor) without disturbing the probe. Collection of unreacted peptide substrate and product peptides by microdialysis using a membrane with a suitable molecular weight cutoff protects collected peptides from enzymatic activity.

Here, we demonstrate that the EOP-MD probe with cLC-MS^2 can measure dose-dependent effects of the inhibitor HFI-419[77] on LE hydrolysis. HFI-419 is a specific inhibitor of insulin-regulated aminopeptidase (IRAP, EC 3.4.11.3), an ectopeptidase known to hydrolyze neuroprotective peptides including the enkephalins,[78,79] arginine-vasopressin,[78,80,81] and oxytocin[78,81] in vitro. These measurements were performed in the rat neocortex, an area of the brain in which both IRAP[82,83] and LE[84,85] are found. This work is novel both technologically and biochemically. It is the first account of using direct laser writing to fabricate a perfusion/sampling device for use in tissue. The probe itself and the accompanying analytical method represent a generic approach for investigating a variety of peptide-related questions in the extracellular space of the brain, and it is the first demonstration of IRAP hydrolysis of a natural peptide substrate in the presence and absence of a specific IRAP inhibitor in vivo.

EXPERIMENTAL SECTION

Direct Laser Writing of the EOP-MD Probe Body.

The probe body consists of three main parts (see Figure 1): the inlet section has cavities to guide the capillaries supporting flow of perfusate, the outlet section is a pointed shaft inside of which are channels for perfusate flow on its way to the outlet ports, and a tube for microdialysis probe mounting and alignment. The overall maximum dimensions of the

probe are 2023 μm (W) × 1015 μm (L) × 3650 μm (H). The outlet ports are 50 μm in diameter. The narrow shaft of the probe (containing the outlet ports) is 150 μm wide and 850 μm long. The microdialysis probe holder had a diameter of 310 μm. See Figure 1. The pattern for perfusion probe was designed in Solidworks and printed by 3D direct laser writer (Nanoscribe Photonic Professional, GT) with IP-S resist. The printing was done through two-photon polymerization of IP-S resist by a femtosecond pulsed laser at 780 nm.

EOP-MD Probe Assembly.

The competing attributes of size and fragility of capillaries was solved by designing the probe to accept fragile 150 mm OD capillaries as inlets and then attaching a more robust 360 mm OD capillary to the narrower capillaries (Figure 1). One-centimeter long sections of 75 μm ID × 150 μm OD capillary (Polymicro) were cut then pushed into the inlet channels of probe until they could go no further. Then, a 15 cm length of 200 μm ID × 360 μm OD capillary was threaded over the top of the 75 μm ID capillary to a distance approximately 0.5 cm from the start of the EOP tip, leaving a 0.5 cm portion of the 75 μm ID capillary exposed. A drop of 2-ton epoxy (Devcon) was placed onto the exposed portion of the 75 μm ID capillary and the 200 μm ID capillary was immediately pushed over the glue and into the EOP probe channel. The EOP probe channel is tapered so that the 200 μm ID capillary can only advance 1 mm into the channel. Applying the glue in this way serves to seal the junction between the 75 μm ID capillary and the 200 μm ID capillary and to seal the area between the 200 μm ID capillary and the channel of the EOP tip. After the epoxy has cured completely, each channel is tested for leaks by flushing the capillaries with water via a syringe. Microdialysis probes (216 μm o.d., 1 mm in length) were assembled using hollow fiber dialysis membrane (Spectra-Por RC Hollow Fiber; MWCO = 13 kDa, 200 μm i.d., Spectrum Laboratories, Inc.; Rancho Dominguez, CA) and fused silica capillaries (40 μm i.d., 100 μm o.d.) using standard procedures described previously.[86]

Generating Electroosmotic Flow.

A complete description of the following can be found in Supporting Information and in Figure 2 in the Results and Discussion section. A plastic centrifuge tube (3 cm (Fisher)) was used to contain modified Ringer's solution (148 mM NaCl (EMD-Millipore, Darmstadt, Germany), 2.7 mM KCl (Sigma-Aldrich), and 0.85 mM $MgCl_2$ (Fisher Scientific) adjusted to a pH of 7.4). The fluidic path for the peptide substrate-containing solution included a short piece of Nafion tubing. The Nafion-containing portion of the (mostly) fused-silica capillary-based fluidic path passed through the modified Ringer's solution. A silver wire electrode in the modified Ringer's solution attached to a suitable current source introduced positive current. The current path went to the EOP-MD probe, through the sample (gel or tissue), through the microdialysis membrane, and out a similar Nafion junction in the dialysate stream flowing to the microdialysis probe.

Quantitative Analysis of Samples.

Except for the use of a more efficient peptide labeling scheme described below, the peptide concentrations in the dialysate were determined using LC-MS^2 as described in an earlier publication[87] and detailed in Supporting Information.

Offline Labeling.

Heavy peptide standards were prepared prior to the experiment using an offline dimethylation procedure adapted from the on-column approach described previously.[88] Stock solutions of LE (American Peptide, Sunnyvale, CA), GGFL (American Peptide), yaGfl (GL Biochem, Shanghai, China), and yasfl (Shanghai Royobiotech, Shanghai, China) were prepared by diluting each solid to a concentration of 1.0 mM in water purified using a Millipore Milli-Q Synthesis A10 filtration system (Billerca, MA). Serial dilutions were then performed until a concentration of 5.3 nM was obtained for each peptide. An aliquot of 49.6 μL of each peptide was then added to an autosampler vial (Thermo Scientific, Rockwood, TN) along with 2 μL of glacial acetic acid (Fisher Chemical, Fair Lawn, NJ). Multiple vials were prepared simultaneously then frozen at −20 °C until needed. On the day of an experiment, a vial was thawed and a volume of 8.0 μL of 4% formaldehyde-d_2 (Sigma-Aldrich, St. Louis, MO) were added, and the mixture was vortexed. Next, 8.0 μL of 600 mM sodium cyanoborohydride (Sigma-Aldrich) were added to the autosampler vial, vortexed, and allowed to react for 5 min. The reaction was then quenched with the addition of 32.0 μL of 1% ammonium hydroxide (Sigma-Aldrich), vortexed again, and allowed to react for 1 min. Finally, 16.0 μL of 5% formic acid (Sigma-Aldrich) were added to the autosampler vial, after which the mixture was vortexed a final time and placed in the refrigerated autosampler at 5 °C. The final concentration of each peptide in the sample was 1.0 nM.

Online Labeling.

Briefly, at the start of each analysis, 1.1 μL of the “heavy-labeled standard” (prepared as described in the previous section) were injected onto the column via the autosampler. Next, 1.1 μL of dialysate were injected onto the column via the “sample valve” housed in the LC oven. Primary amines in the dialysate, retained at the head of the column due to the weak solvent at the beginning of the gradient, were “light” labeled using an on-column procedure described in detail previously.[87] The light labeling reagent, consisting of 350 μL of triethylammonium acetate (100 mM triethyl amine (Sigma-Aldrich) titrated with 100 mM acetic acid to a pH of 7.4), 3.50 μL of 0.6 M sodium cyanoborohydride, and 3.50 μL of 4% formaldehyde (J. T. Baker, Phillipsburg, NJ), was then injected onto the column followed by 5% formic acid. Each reagent was injected at a volume of 1.1 μL. Each chromatogram thus has an internal standard (“heavy-labeled standard”) with a known concentration of each sought-for peptide for use in correcting for ionization efficiency. The ratio of the peak area of a sought-for peptide to its heavy-labeled standard is quantitatively related to the concentration of the sought-for peptide in the injected sample.

In Vivo Sampling.

The EOP-MD probe was soaked in 70% ethanol (Decon, King of Prussia, PA) for 20 min. A solution of 100 nM yasfl in Modified Ringer’s was then perfused through the microdialysis probe at a flow rate of 0.5 μL/min using a Harvard Apparatus PHD 4400 programmable syringe pump (Holliston, MA). The inclusion of yasfl in the perfusate served as a control to ensure the MD probes were working as expected.[87] One channel of the EOP portion of the probe was filled with a solution of 10 μM LE and yaGfl in Modified Ringer’s while the

other channel was filled with a Modified Ringer's solution also containing 10 μM LE and yaGfl as well as the HFI-419 IRAP inhibitor (a gift from Dr. Philip Thompson at Monash University). The HFI-419 concentration (10, 25, and 50 μM) was varied between each rat (n = 3). To check for the presence of bubbles, the probe was lowered into a one-dram vial containing Modified Ringer's and current was applied for 5 min for each channel. Absence of current as voltage is applied is indicative of a bubble. Once it was apparent that the current was sufficiently stable, the current was turned off and the probe lowered into the neocortex. Flow was continuous through the microdialysis probe during insertion. After 1.5 h, the current from the high voltage power supply was turned on and infusion of the peptide solution without inhibitor began. A waiting period was necessary to achieve steady state between the tissue and the microdialysis probe as well as a stable baseline. Sampling occurred for 35 min prior to the first injection and was continuous for 2 h after which the current was stopped, and the electrode moved to the second (peptide + inhibitor) channel. Current was then applied for another 2 h, after which the electrode was moved back to the peptide channel. Sampling then continued for another hour.

In Vivo Data Analysis.

For each rat, five baseline measurements (no inhibitor) were recorded followed by five measurements in the presence of inhibitor (at either 10, 25, or 50 μM). The no-inhibitor and presence-of-inhibitor data were separated by a time of 38 min (two samples) to account for the solution exchange to occur in the brain. The relative area for each peptide was determined by taking the peak area of the light peptide (from dialysate) and dividing it by the peak area of the 1.0 nM heavy peptide standard. The relative area was then converted to a concentration using the calibration curves (see example in Figure S1). Statistical inferences were from Excel and Stata 15.0.

RESULTS

Development of the EOP-MD Probe.

The probe body has two functions: to provide a source of peptide substrate and to hold a microdialysis probe nearby (Figure 1. See also Figure S2 which shows images analogous to Figure 1C in stages of assembly and S3 showing the body represented in Figure 1A, respectively). The source side of the body has two microfluidic channels at the bottom (under the dashed line labeled 'b' in Figure 1a) so that solutions with substrate only and substrate plus inhibitor can be used alternately in the same experiment. The solutions enter the microfluidic channels from fused silica capillaries, Figure 1A. Figure 1B illustrates the layout of the conduits for the capillaries and the microfluidic channels. The distance between the source tip and the nearest surface of the microdialysis probe is controlled by having a tubular element on the side of the EOP-MD body to hold the microdialysis probe (Figure 1A, right). The distal portion of a fully constructed EOP-MD probe is shown as Figure 1C. The source probe (Figure 1A, right pair of images) is not cylindrical. The wider dimension in the untapered section (see label c in Figure 1A) is designed to be 200 μm wide, while the narrower dimension is designed to be 125 μm. The latter outer dimension as measured using a stereoscope was 120 ± 5 μm (mean ± SEM, n = 3). The former

was measured (Figure S3) to be 180 ± 5 μm. Optical images from stages of preparing the finished EOP-MD probe from the parts are shown in Figure S2.

Electroosmotic delivery was achieved using a constant current. Figure 2 illustrates that the fluid supporting the electrochemical reactions is separated from the peptide-containing solution by a tubular Nafion membrane. Cations transport the current through the Nafion. The positive ionic current passes through the source capillary to the body of the probe, out the probe tip, through the medium (tissue or gel), through the microdialysis membrane, and through the inlet microdialysis capillary exiting at a second Nafion membrane/electrode apparatus. The current passes through about 8 cm of capillary tubing on its way to the EOP probe body and the same length coming out of the brain. Details on the construction of this device are in SI, section S2.1.

In Vitro Fluorescence Studies.

To visualize solute transport from the perfusion tip to the MD probe, we infused 3 kDa Texas Red (TR3), which is neutral, and tris(bipyridyl)-Ru(II) ($Ru(bpy)_3^{2+}$) into a piece of hydrogel with a ζ potential similar to the brain's[89] and monitored the fluorescence intensity over time. Figure 3a is a brightfield image of the EOP-MD probe positioned in the gel. Figures 3b and c demonstrate the fluorescence before and after perfusion of TR3 for 5 min at 75 μA. The corresponding false color plots, 3d and e, illustrate the solute's presence in the region of hydrogel between the source opening and the microdialysis membrane. At longer times, more solute permeates the hydrogel because only a fraction is taken up by the microdialysis probe (Figure S4). Details on hydrogel synthesis and fluorescence measurements can be found in SI sections S2.2 and 2.3.

Assessing Mass Transport with yaGfl.

In the assessment of enzymatic degradation of a peptide traversing the extracellular space, it is necessary to have an internal standard representing what would be observed in the absence of enzymatic activity. The peptidase-resistant D-amino acid yaGfl (N.B., we use the convention that (except for glycine) the upper-case, single-letter abbreviation of the amino acids implies the L optical isomer, and lower case implies the D optical isomer) has not shown any measurable hydrolysis in OHSCs in analogous experiments.[51,52,55,56] We first examined transport of LE and yaGfl in vitro. A solution containing 10 μM LE and yaGfl was infused electroosmotically with the EOP-MD probe in a hydrogel. Peptide concentrations in dialysate were determined by LC-MS^2. (Details including masses of sought-for ions are in section S2.4 of SI.) A second D-amino acid peptide, yasfl, was in the dialysate. This was used qualitatively to confirm microdialysis probe function. We found no significant difference between the concentrations of LE and yaGfl in the dialysate at either of two currents, 15 and 30 μA (Figure 4a). We further validated yaGfl as an internal standard in vivo in an anesthetized rat. (For details of surgery, see SI, section S2.5. For probe placement, see Figure S5.) There was no significant difference ($p < 0.05$) between the yaGfl concentrations in the dialysate in vivo compared to in vitro (Figure 4b). We infused 10 μM LE and yaGfl in vivo and observed a statistically significant increase in the dialysate concentration of yaGfl upon increasing current from 5 to 15 μA ($p < 0.01$), as well as from 15 μA to 30 μA ($p < 0.05$) (Figure 4C). This is attributable to the increase in the Péclet

number as current increases. There was also a statistically significant difference between [LE] in the dialysate compared to [yaGfl] at each current.

We define the collection efficiency as the ratio of the mass flow rate (mol/s) of an infused substance, such as yaGfl, collected by the microdialysis probe to the mass flow rate of that substance infused by electroosmotic flow. Note that this is different from ordinary practice where concentrations are used. Figure 5 illustrates the collection efficiency versus the inverse of the current. The collection efficiency of the hydrolyzable LE and that of yaGfl depend on current in qualitatively different ways. The average time an unreactive solute spends in the tissue between the source and the microdialysis probe (the residence time in the tissue) is related to the inverse of the current. The collection efficiency of the reactive LE decreases as residence time increases as expected because it is hydrolyzed. The collection efficiency of the inert yaGfl increases with residence time. The difference in the two collection efficiencies as a function of residence time is clearly indicative of the loss of LE. To achieve the dynamic range to detect changes in both LE and GGFL reliably, we used the intermediate current, 15 μA, for subsequent inhibitor experiments. This current is also in a range that we have determined is minimally harmful to tissue.[90]

LE Hydrolysis in the Presence and Absence of HFI-419.

We sought to determine whether there was an effect of HFI-419,[77] a specific IRAP inhibitor, on the hydrolysis of LE. To be consistent with our EOP-MD experiments described above, we perfused 10 μM LE and yaGfl in the presence and absence of 10, 25, and 50 μM HFI-419. The product, GGFL is itself subject to hydrolysis by ectopeptidases. Thus, the quantitative measure of the extent of reaction is the fractional loss of substrate, $([S_0] - [S])/[S_0]$ where $[S_0]$ is initial substrate concentration and [S] is detected substrate concentration. Figure 6 shows statistically significant decreases in $([S_0] - [S])/[S_0]$ at each step increase in inhibitor concentration: From 0 ($n = 15$) to 10 μM ($n = 5$; $p = 0.0028$, *t* test with equal variances assumption based on F-test), from 10 to 25 μM ($n = 5$ each; $p = 0.012$, *t* test with unequal variances based on F-test), and from 25 to 50 μM ($n = 5$ each; $p = 0.0017$, *t* test with equal variances assumption based on F-test)

DISCUSSION

Electroosmotic perfusion is effective in vivo. Regarding the device itself, as described above, previously, we demonstrated the utility of this approach to analysis of extracellular processes in brain using organotypic hippocampal cultures with a single collection probe and substrate in the medium,[51,54] or in a push–pull arrangement[52,53,56] with analysis by MALDI MS,[52] online by CE on a microfluidic device,[54] or offline using capillary LC[51] to study the degradation of enkephalins,[51,56] galanin,[52] and coenzyme A.[54] Attempts to mimic the push–pull perfusion with a separate source probe and a microdialysis probe failed because of the inability to position the pair accurately. Thus, we devised the device described here to solve this problem. Both in vivo and in vitro the device appears to function as intended: the space between the source and the probe's outer surface does fill with the infused solute, and enzymatic reactions occur in that space in vivo. The arrangement of the electrodes—using the inlet and outlet microdialysis capillaries to carry the current—is effective. The

reproducibility both in vitro and in vivo is acceptable based on the relative uncertainties shown in Figures 4–6 (the 0 inhibitor data).

To be sure, this approach has limitations. One that it shares with all microdialysis measurements is tissue damage.[91] Another is that the perfusion process required about 40 min after changing from infusion of inhibitor-free fluid to inhibitor-containing fluid to achieve a representative measurement of the steady-state concentration of measured substrate. A third is that, like its predecessor EOPPP,[55] the infusion process leads to a dilution of the infused substances. We estimate based on the recovery of the substrate analog, yaGfl, and the microdialysis extraction of yasfl that the concentration in the tissue resulting from infusing a 10 μM concentration of yaGfl is on the order of a few hundred nM. Furthermore, as readily seen in Figure 3, the concentration of an infused substance is not homogeneous. In order to provide even more quantitative detail, simulations analogous to those done for EOPPP[55] will be necessary. Simulations would also lend support to our hypothesis that the measurements are sensitive to enzyme activity in the region between the source and the microdialysis probe. As for the range of peptide substrates that could be investigated, the major limitation is the electrophoretic mobility of the peptide. Anionic peptides that have an electrophoretic mobility with a magnitude (absolute value) similar to the electroosmotic mobility cannot be studied. Regardless of the sign of the current, such peptides would experience no net force in the presence of a current in brain tissue. For many biologically relevant peptides in the size range beyond five or so amino acids, even anionic peptides, the electroosmotic flow dictates the direction of motion in an electric field.

Regarding the overall method, there are a few observations. An internal standard is necessary. To infer relative values of enzyme activity, for example, in the presence and absence of inhibitor, the ratio of product to initial substrate concentration is needed.[55,92] We use yaGfl to infer the amount of substrate that would have been recovered in the absence of hydrolysis. Figure 4 shows that the collected yaGfl concentration was not statistically distinguishable from that of LE in vitro. Thus, yaGfl has similar electroosmotic transport through the hydrogel as LE. The concentration of yaGfl collected in the in vivo experiments was not significantly different from that in the in vitro experiment. The collected yaGfl levels are a suitable substitute for the concentration of LE that would be recovered in the absence of hydrolysis in the brain, S_0. On the other hand, the concentrations of LE and yaGfl in Figure 4c are significantly different at each current used in vivo. We attribute this difference to LE hydrolysis in the tissue. Accordingly, we detected the major product, GGFL. The sum of the concentrations of LE and GGFL do not equal that of yaGfl, indicating that GGFL is further hydrolyzed or that other products are formed from YGGFL. As the quantitative analysis of LE hydrolysis in the presence/absence of inhibitor was our goal, we did not determine which other products were formed from LE or GGFL.

While electroosmosis (and electrophoresis for a charged solute) brings solute into the tissue, mass transport by diffusion in the tissue is important. This observation is consistent with simulations on a related technique applied to organotypic cultures[93] and the images obtained in hydrogels here. Further evidence comes from the extraction fraction, E, of the *microdialysis* internal standard, yasfl. Significantly altering the fluid flow rate past the microdialysis probe's exterior surface would increase E. Experimentally, we observe that E

for yasfl is independent of current. This implies that mass transport by electroosmotic fluid flow is not dominant near the microdialysis probe, thus diffusional mass transport near the probe is important.

The effect of current on collection efficiency distinguishes reactive solutes that are lost in the tissue from unreactive solutes (Figure 5). We determine the collection efficiency based on well-known experimental parameters. The mass flow rate of a solute into the tissue is the product of the fluid flow rate in the tissue and the solute concentration. The ratio of electroosmotic flow rate to current in the tissue is 1.45×10^{-8} m^3 A^{-1} s^{-1} or 0.87 nL/min per μA in more practical terms.[49,55] The concentrations of yaGfl and LE in the source are each 10 μM. Thus, for example, at a current of 15 μA, the mass flow into the tissue is 2.2 fmol/s. Turning to the other end of the problem, the volume flow rate of the microdialysate through the lumen of the probe is 0.5 μL/min and the concentration of yaGfl is determined by LC-MS (in the tens of nM range). The measured concentration in the dialysate and the microdialysate flow rate yield a value for the mass flow rate of captured peptide. The ratio of captured to infused mass flow rate is the collection efficiency.

Figure 5 shows the collection efficiencies in vivo for both LE and yaGfl. For yaGfl, the increase is not linear. This is expected. In prior work[49] we showed that electrokinetic delivery from a small orifice yields a concentration-distance profile that depends on the current density applied. Approximate calculations show that a change the current by a factor of 6 (from 30 to 5 μA) results in a change in the concentration (of an unreactive species) near the microdialysis membrane of less than 2-fold (see Supporting Information). The ratio of mass/time collected (in the dialysate) to mass/time delivered (into the brain) is the collection efficiency. Let us say that the collection efficiency is C with a current of 30 μA. Decreasing current by a factor of 6 decreases mass/time delivered by the same factor. At the same time mass/time collected in dialysate decreases 2-fold. The collection efficiency is then $2C/6$, a decrease of about a factor of 3. *Decreasing* current (*increasing* residence time) increases collection efficiency of an unreactive species. Experimentally, Figure 4C shows that as current decreases six times the experimental yaGfl collection efficiency increases only a factor of 2.6, consistent with the approximate calculation. The reactive LE, on the other hand, demonstrates that a longer residence time in the tissue causes a greater extent of hydrolysis.

The optimum current depends on the application. Qualitatively, we can use Figure 5 to determine the appropriate current to use in a certain case. Because we are interested in the effect of a peptidase inhibitor, it is appropriate to use conditions leading to a significant loss of substrate in the tissue in the absence of inhibitor. Perfusing with 15 μA achieves this under the conditions used here. In observing a process that would decrease the substrate concentration, such as upregulation of the ectopeptidase, a higher current, and thus higher substrate recovery, would be beneficial so that a decrease could be quantitated.

The probe design could be improved. The exposed area of the microdialysis probe on the side away from the source just adds background solutes. Refining the active area of the probe and its length dimension based, for example, on simulations would improve the signal to background ratio. Alternatively, the source could have multiple ports to deliver solute

along a length corresponding to the exposed length of the microdialysis probe. (Thanks to Reviewer 1 for this suggestion.) The limitation on the number and size of source ports is the total current required. In passing through narrow channels there will be Joule heating. This is a manageable problem but because there are so many parameters to consider, simulation is again the best way to determine how to design such a source.

The presence of multiple ectopeptidases makes measurement of substrate loss the best approach to determining changes in overall ectoenzyme activity. For example, at 15 μA the sum of the concentrations of LE and GGFL is less than the concentration of yaGfl (Figure 4c). There are two contributions to this apparent discrepancy: GGFL is itself hydrolyzed and YGGFL is hydrolyzed by other enzymes. YGGFL is hydrolyzed by neprilysin to YGG and FL, although its relative activity in the cortex is reported to be low.[94] It is also hydrolyzed by aminopeptidase N to Y and GGFL. While autoradiography shows the presence of aminopeptidase N in the cortex,[95] MALDI imaging found little activity in the region of the cortex investigated here.[96] We note that GGFL was detected in experiments without inhibitor but was undetected during infusion of 50 μM HFI-419 (data not shown). The simplest explanation is that the major source of GGFL is by IRAP's actions on LE. This implies that hydrolysis at the Y-G bond by other ectoenzymes is not significant, and that the "missing" YGGFL may be caused by hydrolysis at the G-F bond by neprilysin (EC 3.4.11.22). Clearly, the analysis of a broader spectrum of peptides would help to elucidate more details. Despite the lack of information on these other ectopeptidases, the selectivity of the approach depends upon measuring the *change* in observed loss of substrate as a selective inhibitor concentration is changed. This permits distinguishing IRAP activity from other enzymatic activity.

CONCLUSION

The EOP-MD probe and methods are effective in determining changes in enzyme activity in vivo in the presence of an inhibitor. The measured concentration of a D-amino acid analog of the substrate acts as a surrogate for the concentration of substrate that would be recovered in the absence of the enzyme reaction. This permits the quantitative evaluation of the effect of an inhibitor on the ectoenzyme reaction. The EOP-MD probe and accompanying method provide important insight into the hydrolysis of LE by the ectopeptidase HFI-419. We are able to quantify the fraction of substrate lost under conditions of different average substrate residence times. Future work will include looking for a broader range of peptides to identify the other hydrolysis reactions occurring in parallel with the sought-for ectoenzyme, decreasing analysis time to obtain more data points per time, and simulating the process[55] to further refine our understanding.

Supplementary Material

Refer to Web version on PubMed Central for supplementary material.

ACKNOWLEDGMENTS

A gift of HFI-419 from Prof. Philip E. Thompson, The University of Melbourne, is gratefully acknowledged. Very helpful conversations with Dr. Benjamin Richter at Nanoscribe are gratefully acknowledged. This work was supported by the National Institute of General Medical Sciences through grant R01 GM044842.

REFERENCES

(1). Konkoy CS; Davis TP Trends Pharmacol. Sci 1996, 17, 288–294. [PubMed: 8810875]

(2). Murphy NP ACS Chem. Neurosci 2015, 6, 94–107. [PubMed: 25585132]

(3). van den Pol AN Neuron 2012, 76, 98–115. [PubMed: 23040809]

(4). Antczak C; De Meester I; Bauvois B BioEssays 2001, 23, 251–260. [PubMed: 11223882]

(5). Ban L; Pettit N; Li L; Stuparu AD; Cai L; Chen W; Guan W; Han W; Wang PG; Mrksich M Nat. Chem. Biol 2012, 8, 769–773. [PubMed: 22820418]

(6). Yates NA; Deyanova EG; Geissler W; Wiener MC; Sachs JR; Wong KK; Thornberry NA; Sinha Roy R; Settlage RE; Hendrickson RC Int. J. Mass Spectrom 2007, 259, 174–183.

(7). Bothner B; Chavez R; Wei J; Strupp C; Phung Q; Schneemann A; Siuzdak G J. Biol. Chem 2000, 275, 13455–13459. [PubMed: 10788458]

(8). Sun L; Stenken JA; Yang AY; Zhao JJ; Musson DG Anal. Biochem 2007, 370, 26–37. [PubMed: 17765862]

(9). Van Noorden CJF J. Histochem. Cytochem 2010, 58, 481–497. [PubMed: 20124092]

(10). Vandooren J; Geurts N; Martens E; Van den Steen PE; Opdenakker G Nat. Methods 2013, 10, 211–220. [PubMed: 23443633]

(11). Bivehed E; Stroemvall R; Bergquist J; Bakalkin G; Andersson M Peptides (N. Y., NY, U. S.) 2017, 87, 20–27.

(12). Grobe N; Elased KM; Cool DR; Morris M Am. J. Physiol 2012, 302, E1016–E1024.

(13). OuYang C; Chen B; Li L J. Am. Soc. Mass Spectrom 2015, 26, 1992–2001. [PubMed: 26438126]

(14). Hingorani DV; Yoo B; Bernstein AS; Pagel MD Chem. - Eur. J 2014, 20, 9840–9850. [PubMed: 24990812]

(15). Wienkers LC; Heath TG Nat. Rev. Drug Discovery 2005, 4, 825–833. [PubMed: 16224454]

(16). Ungerstedt U; Hallström Å Life Sci 1987, 41, 861–864. [PubMed: 2886879]

(17). Wang Y; Zagorevski DV; Stenken JA Anal. Chem. (Washington, DC, U. S.) 2008, 80, 2050–2057.

(18). Maidment NT; Siddall B; Rudolph VD; Evans CJ J. Neurochem 1991, 56, 1980–1984. [PubMed: 2027009]

(19). André PE; Caprioli RM J. Mass Spectrom 1995, 30, 817–824.

(20). Kostel KL; Lunte SM J. Chromatogr., Biomed. Appl 1997, 695, 27–38.

(21). Zhang H; Stoeckli M; Andren PE; Caprioli RM J. Mass Spectrom 1999, 34, 377–383. [PubMed: 10226364]

(22). Freed AL; Cooper JD; Davies MI; Lunte SM J. Neurosci. Methods 2001, 109, 23–29. [PubMed: 11489296]

(23). Reed B; Zhang Y; Chait BT; Kreek MJ J. Neurochem 2003, 86, 815–823. [PubMed: 12887680]

(24). Stragier B; Sarre S; Vanderheyden P; Vauquelin G; Fournie-Zaluski M-C; Ebinger G; Michotte Y J. Neurochem 2004, 90, 1251–1257. [PubMed: 15312180]

(25). Klintenberg R; Andren PE J. Mass Spectrom 2005, 40, 261–270. [PubMed: 15706626]

(26). Reed B; Bidlack JM; Chait BT; Kreek MJ J. Neuroendocrinol 2008, 20, 606–616. [PubMed: 18363801]

(27). Beyer CE; Dwyer JM; Platt BJ; Neal S; Luo B; Ling H-P; Lin Q; Mark RJ; Rosenzweig-Lipson S; Schechter LE Psychopharmacology (Heidelberg, Ger.) 2010, 209, 303–311.

(28). Sato T; Obata T; Yamanaka Y; Arita M Br. J. Pharmacol 1998, 125, 493–498. [PubMed: 9806332]

(29). Obata T Life Sci 2002, 71, 2083–2103. [PubMed: 12204768]
(30). Sandeep TC; Andrew R; Homer NZM; Andrews RC; Smith K; Walker BR Diabetes 2005, 54, 872–879. [PubMed: 15734867]
(31). Mou X; Stenken JA Anal. Chem 2006, 78, 7778–7784. [PubMed: 17105171]
(32). Sun L; Stenken JA; Brunner JE; Michel KB; Adelsberger JK; Yang AY; Zhao JJ; Musson DG Anal. Biochem 2008, 381, 214–223. [PubMed: 18638442]
(33). Wen X-D; Yang J; Ma R-H; Gao W; Qi L-W; Li P; Bauer BA; Du G-J; Zhang Z; Somogyi J; Wang C-Z; Yuan C-S J. Chromatogr. B: Anal. Technol. Biomed. Life Sci 2012, 895–896, 162–168.
(34). Wang L; Pi Z; Liu S; Liu Z; Song F Sci. Rep 2017, 7, 1–11. [PubMed: 28127051]
(35). Morrison PF; Bungay PM; Hsiao JK; Ball BA; Mefford IN; Dedrick RL J. Neurochem 1991, 57, 103–119. [PubMed: 2051160]
(36). Bungay PM; Morrison PF; Dedrick RL Life Sci 1990, 46, 105–119. [PubMed: 2299972]
(37). Yang H; Peters JL; Allen C; Chern S-S; Coalson RD; Michael AC Anal. Chem 2000, 72, 2042–2049. [PubMed: 10815963]
(38). Chen KC; Hoistad M; Kehr J; Fuxe K; Nicholson C J. Neurochem 2002, 81, 94–107. [PubMed: 12067242]
(39). Wang Y; Zagorevski DV; Lennartz MR; Loegering DJ; Stenken JA Anal. Chem. (Washington, DC, U. S.) 2009, 81, 9961–9971.
(40). Steuerwald AJ; Villeneuve JD; Sun L; Stenken JA J. Pharm. Biomed. Anal 2006, 40, 1041–1047. [PubMed: 16242888]
(41). Chen MY; Lonser RR; Morrison PF; Governale LS; Oldfield EH J. Neurosurg 1999, 90, 315–320. [PubMed: 9950503]
(42). Altenbach M; Schnyder N; Zimmermann C; Imanidis G Int. J. Pharm 2006, 307, 308–317. [PubMed: 16310991]
(43). Raiman J; Koljonen M; Huikko K; Kostiainen R; Hirvonen J Eur. J. Pharm. Sci 2004, 21, 371–377. [PubMed: 14757511]
(44). Chiang C-H; Shao C-H; Chen J-L Drug Dev. Ind. Pharm 1998, 24, 431–438. [PubMed: 9876605]
(45). Harding JW; Felix D Brain Res 1987, 424, 299–304. [PubMed: 3676828]
(46). Pritchett JS; Shippy SA J. Chromatogr. B: Anal. Technol. Biomed. Life Sci 2014, 955–956, 81–85.
(47). Guy Y; Sandberg M; Weber SG Biophys. J 2008, 94, 4561–4569. [PubMed: 18263658]
(48). Guy Y; Muha RJ; Sandberg M; Weber SG Anal. Chem 2009, 81, 3001–3007. [PubMed: 19298057]
(49). Guy Y; Faraji AH; Gavigan CA; Strein TG; Weber SG Anal. Chem 2012, 84, 2179–2187. [PubMed: 22264102]
(50). Dubey S; Kalia YN J. Controlled Release 2011, 152, 356–362.
(51). Xu H; Guy Y; Hamsher A; Shi G; Sandberg M; Weber SG Anal. Chem 2010, 82, 6377–6383. [PubMed: 20669992]
(52). Rupert AE; Ou Y; Sandberg M; Weber SG ACS Chem. Neurosci 2013, 4, 838–848. [PubMed: 23614879]
(53). Rupert AE; Ou Y; Sandberg M; Weber SG ACS Chem. Neurosci 2013, 4, 849–857. [PubMed: 23639590]
(54). Wu J; Sandberg M; Weber SG Anal. Chem 2013, 85, 12020–12027. [PubMed: 24215585]
(55). Ou Y; Weber SG Anal. Chem 2017, 89, 5864–5873. [PubMed: 28447456]
(56). Ou Y; Weber SG ACS Chem. Neurosci 2018, 9, 535–544. [PubMed: 29078045]
(57). Ou Y; Wu J; Sandberg M; Weber SG Anal. Bioanal. Chem 2014, 406, 6455–6468. [PubMed: 25168111]
(58). Silbernagel N; Koerner A; Balitzki J; Jaggy M; Bertels S; Richter B; Hippler M; Hellwig A; Hecker M; Bastmeyer M; Ullrich ND Biomaterials 2020, 227, 119551. [PubMed: 31670034]
(59). Xu H; Medina-Sanchez M; Magdanz V; Schwarz L; Hebenstreit F; Schmidt OG ACS Nano 2018, 12, 327–337. [PubMed: 29202221]

(60). Marino A; Tricinci O; Battaglini M; Filippeschi C; Mattoli V; Sinibaldi E; Ciofani G Small 2018, 14, 1702959.

(61). Aksit A; Arteaga DN; Arriaga M; Wang X; Watanabe H; Kasza KE; Lalwani AK; Kysar JW Biomed. Microdevices 2018, 20, 47. [PubMed: 29884927]

(62). Hong N; Yang GH; Lee J; Kim G J. Biomed. Mater. Res., Part B 2018, 106, 444–459.

(63). Barner-Kowollik C; Bastmeyer M; Blasco E; Delaittre G; Mueller P; Richter B; Wegener M Angew. Chem., Int. Ed 2017, 56, 15828–15845.

(64). Brand CA; Linke M; Weissenbruch K; Richter B; Bastmeyer M; Schwarz US Biophys. J 2017, 113, 770–774. [PubMed: 28755755]

(65). Richter B; Hahn V; Bertels S; Claus TK; Wegener M; Delaittre G; Barner-Kowollik C; Bastmeyer M Adv. Mater. (Weinheim, Ger.) 2017, 29, 1604342.

(66). Di Giacomo R; Krodel S; Maresca B; Benzoni P; Rusconi R; Stocker R; Daraio C Sci. Rep 2017, 7, 45897. [PubMed: 28378786]

(67). Faraji Rad Z; Nordon RE; Anthony CJ; Bilston L; Prewett PD; Arns J-Y; Arns CH; Zhang L; Davies GJ Microsystems & Nanoengineering 2017, 3, 17034. [PubMed: 31057872]

(68). Lissandrello CA; Gillis WF; Shen J; Pearre BW; Vitale F; Pasquali M; Holinski BJ; Chew DJ; White AE; Gardner TJJ Neural Eng 2017, 14, No. 036006.

(69). Son AI; Opfermann JD; McCue C; Ziobro J; Abrahams JH III; Jones K; Morton PD; Ishii S; Oluigbo C; Krieger A; Liu JS; Hashimoto-Torii K; Torii M Sci. Rep 2017, 7, 1–16. [PubMed: 28127051]

(70). Miller PR; Boehm RD; Skoog SA; Edwards TL; Rodriguez M; Brozik S; Brener I; Byrd T; Baca JT; Ashley C; Narayan RJ; Polsky R Electroanalysis 2015, 27, 2239–2249.

(71). Suzuki M; Sawa T; Takahashi T; Aoyagi S In 2015 IEEE/RSJ International Conference on Intelligent Robots and Systems (IROS), 2015; pp 2748–2753.

(72). Greiner AM; Klein F; Gudzenko T; Richter B; Striebel T; Wundari BG; Autenrieth TJ; Wegener M; Franz CM; Bastmeyer M Biomaterials 2015, 69, 121–132. [PubMed: 26283159]

(73). Malinauskas M; Baltriukiene D; Kraniauskas A; Danilevicius P; Jarasiene R; Sirmenis R; Zukauskas A; Balciunas E; Purlys V; Gadonas R; Bukelskiene V; Sirvydis V; Piskarskas A Appl. Phys. A: Mater. Sci. Process 2012, 108, 751–759.

(74). Greiner AM; Richter B; Bastmeyer M Macromol. Biosci 2012, 12, 1301–1314. [PubMed: 22965790]

(75). Klein F; Richter B; Striebel T; Franz CM; von Freymann G; Wegener M; Bastmeyer M Adv. Mater. (Weinheim, Ger.) 2011, 23, 1341–1345.

(76). Yang C; Cao Q; Puthongkham P; Lee ST; Ganesana M; Lavrik NV; Venton BJ Angew. Chem., Int. Ed 2018, 57, 14255–14259.

(77). Albiston AL; Morton CJ; Ng HL; Pham V; Yeatman HR; Ye S; Fernando RN; De Bundel D; Ascher DB; Mendelsohn FA; Parker MW; Chai SY FASEB J 2008, 22, 4209–4217. [PubMed: 18716029]

(78). Lew RA; Mustafa T; Ye S; McDowall SG; Chai SY; Albiston AL J. Neurochem 2003, 86, 344–350. [PubMed: 12871575]

(79). Matsumoto H; Nagasaka T; Hattori A; Rogi T; Tsuruoka N; Mizutani S; Tsujimoto M Eur. J. Biochem 2001, 268, 3259–3266. [PubMed: 11389728]

(80). Herbst JJ; Ross SA; Scott HM; Bobin SA; Morris NJ; Lienhard GE; Keller SR Am. J. Physiol 1997, 272, E600–606. [PubMed: 9142880]

(81). Wallis MG; Lankford MF; Keller SR Am. J. Physiol Endocrinol Metab 2007, 293, E1092–1102. [PubMed: 17684103]

(82). Fernando RN; Luff SE; Albiston AL; Chai SY J. Neurochem 2007, 102, 967–976. [PubMed: 17504262]

(83). Hernandez J; Prieto I; Segarra AB; de Gasparo M; Wangensteen R; Villarejo AB; Banegas I; Vives F; Cobo J; Ramirez-Sanchez M Behav. Brain Res 2015, 287, 42–48. [PubMed: 25819424]

(84). Hughes J; Kosterlitz HW; Smith TW Br. J. Pharmacol 1977, 61, 639–647. [PubMed: 597668]

(85). Gray NW; Weimer RM; Bureau I; Svoboda K PLoS Biol 2006, 4, e370. [PubMed: 17090216]

(86). Mitala CM; Wang Y; Borland LM; Jung M; Shand S; Watkins S; Weber SG; Michael AC J. Neurosci. Methods 2008, 174, 177–185. [PubMed: 18674561]

(87). Wilson RE; Jaquins-Gerstl A; Weber SG Anal. Chem 2018, 90, 4561–4568. [PubMed: 29504751]

(88). Koehler CJ; Arntzen MO; de Souza GA; Thiede B Anal. Chem 2013, 85, 2478–2485. [PubMed: 23316706]

(89). Faraji AH; Cui JJ; Guy Y; Li L; Gavigan CA; Strein TG; Weber SG Langmuir 2011, 27, 13635–13642. [PubMed: 21905710]

(90). Hamsher AE; Xu H; Guy Y; Sandberg M; Weber SG Anal. Chem 2010, 82, 6370–6376. [PubMed: 20698578]

(91). Borland LM; Shi G; Yang H; Michael AC J. Neurosci. Methods 2005, 146, 149–158. [PubMed: 15975664]

(92). Goličnik M J. Enzyme Inhib. Med. Chem 2013, 28, 879–893. [PubMed: 22630075]

(93). Ou Y; Weber SG ACS Chem. Neurosci 2018, 9, 535. [PubMed: 29078045]

(94). Facchinetti P; Rose C; Schwartz JC; Ouimet T Neuroscience 2003, 118, 627–639. [PubMed: 12710972]

(95). Noble F; Banisadr G; Jardinaud F; Popovici T; Lai-Kuen R; Chen H; Bischoff L; Parsadaniantz SM; Fournie-Zaluski MC; Roques BP Neuroscience 2001, 105, 479–488. [PubMed: 11672613]

(96). Bivehed E; Stromvall R; Bergquist J; Bakalkin G; Andersson M Peptides 2017, 87, 20–27. [PubMed: 27840228]

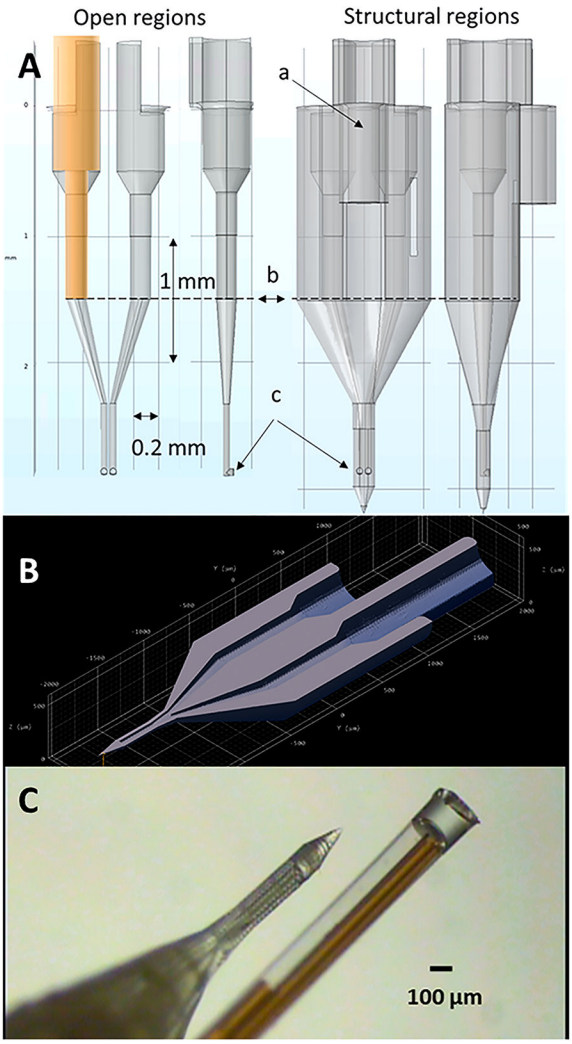

Figure 1.

(A) Drawings of front (left) and side views (second from left) of the open or hollow regions of the probe. The left figure illustrates the inserted 360 and 100 μm capillaries that carry the substrate-containing solutions into the fluidic channels in the probe. The structural regions of the device are shown on the right. Arrow ‘a’ points out the guide for the microdialysis probe, and ‘b’ is a dividing line. Above this line, fluid is carried by capillaries; below, by the fluidic channels. ‘c’ points out the exit holes. (B) View of the channels in a cutaway view of the device. (C) Assembled device.

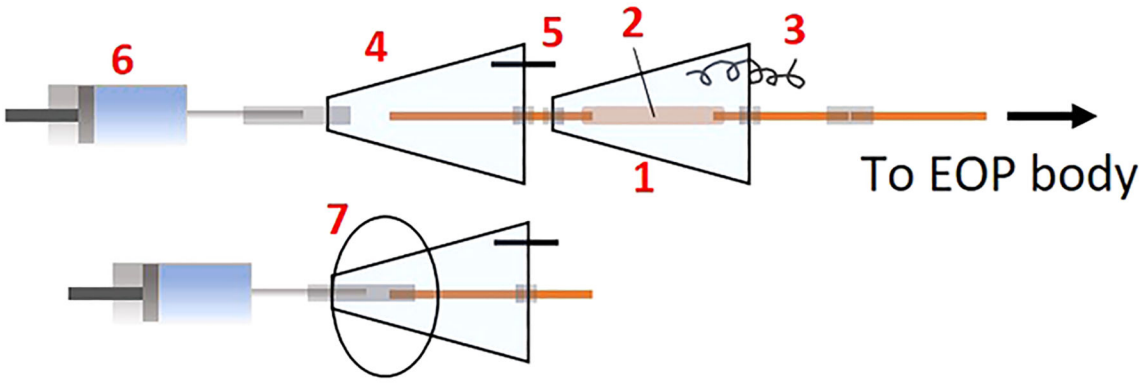

Figure 2.

Schematic illustration of the EOP source apparatus. There are three major components: A current source (1–3), a peptide substrate-containing reservoir (4–5), and a movable filling syringe (6–7). The current source comprises (1) a reservoir containing modified Ringer's solution, (2) Nafion tubing, and (3) a silver electrode. The substrate-containing reservoir (4) is open to the atmosphere through a needle (5). The filling syringe (6) is disengaged from the flow path inside the substrate-containing reservoir (4) during operation. Prior to use, the filling syringe containing the solution to be infused is pushed to engage a sleeve attached to the syringe's needle (7) with the capillary carrying the substrate-containing solution. Following filling, the syringe is disengaged (4). The apparatus is kept approximately horizontal to avoid the effect of gravity.

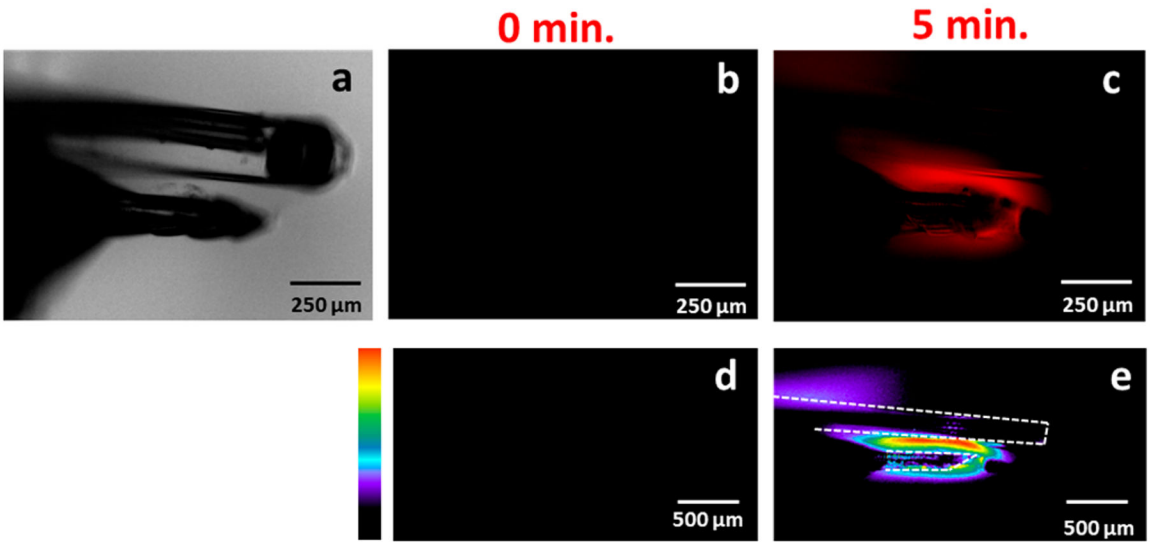

Figure 3.

4× (a) Brightfield and (b, c) fluorescence microscopy images of the perfusion of 3 kDa Texas Red dye into a hydrogel prior to turning on current (0 min, (b)) and after (c) 5 min of perfusion at 75 μA. The corresponding false color plots are shown in panels d and e. The white dashed lines in panel e outlines the source probe tip and the portion of the lumen of the microdialysis membrane that is not occupied by a capillary.

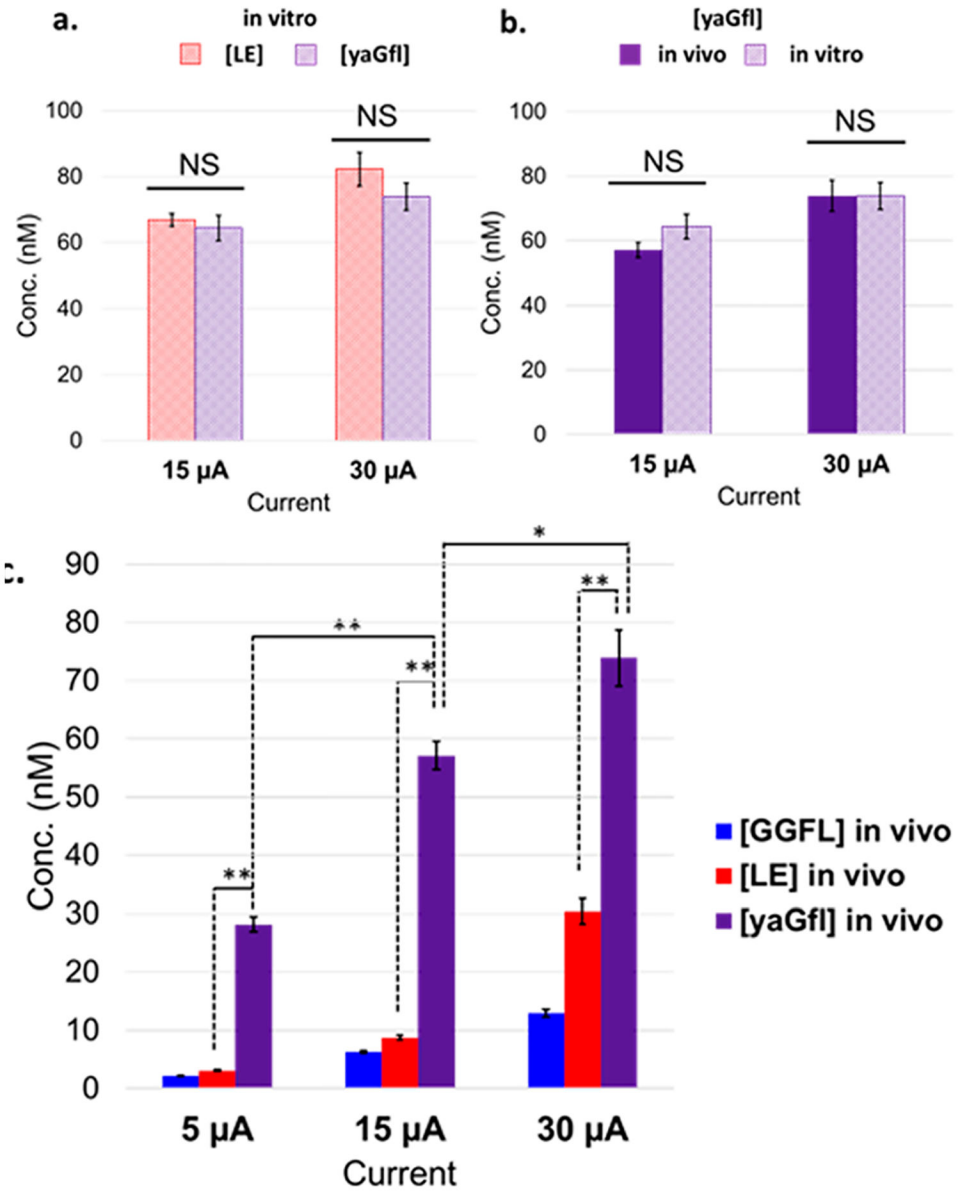

Figure 4.

(a) No significant difference (*t* test) in the concentrations of leu-enkephalin (LE, hatched red) and yaGfl (hatched purple) in dialysate during the electroosmotic perfusion of 10 μM LE and yaGfl in vitro at 15 μA and 30 μA using the EOP-MD device. (b) No significant difference (*t* test) in the concentrations of yaGfl in the dialysate in vivo (dark purple) vs in vitro (hatched purple). Figure 4c depicts the concentrations of GGFL (solid blue bar), LE (solid red bar), and yaGfl measured in the dialysate in in vivo experiments. "NS" indicates that the values shown under the bar were not significantly different as determined by ANOVA ($p > 0.05$) with post hoc Tukey test. The single asterisk (*) and double asterisk (**) represent $p < 0.05$ and $p < 0.01$, respectively. The error bars indicate the SEM for $n = 3$ replicates for in vitro data and $n = 4$. replicates for in vivo data.

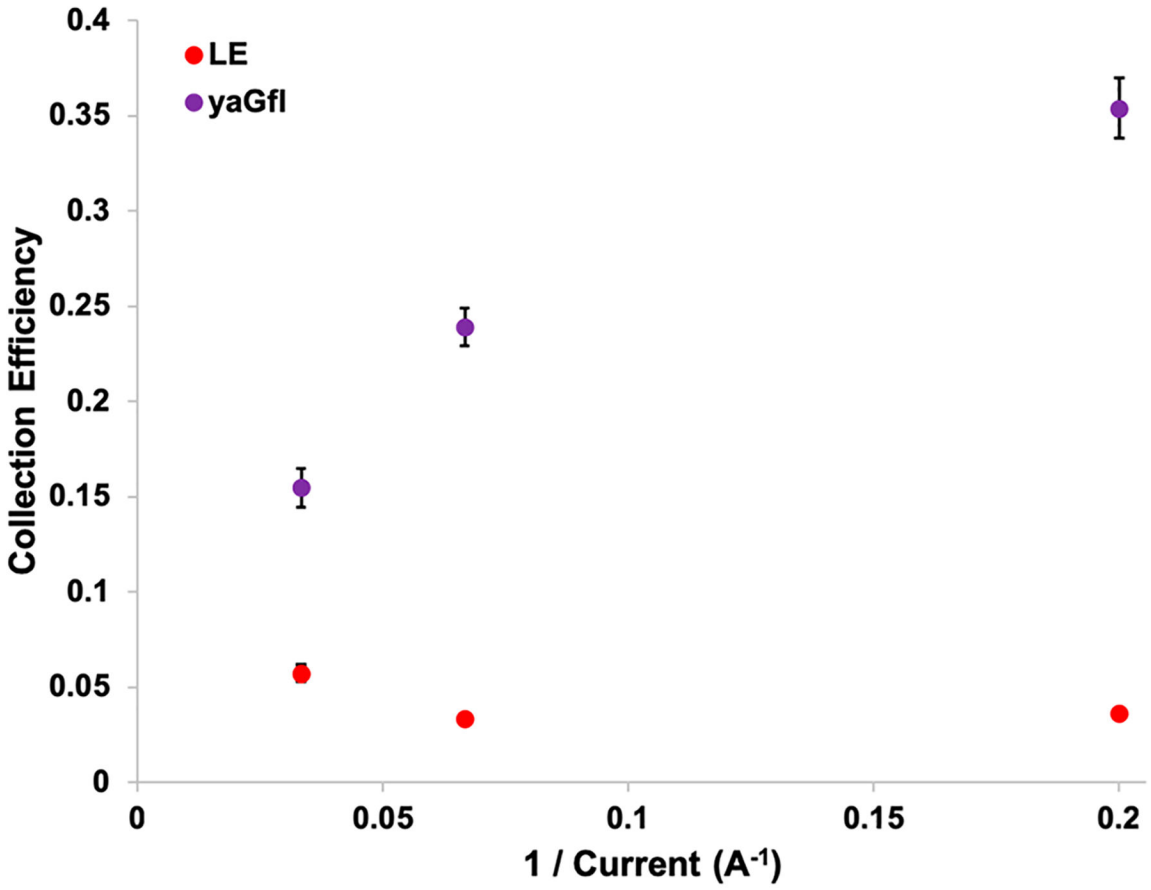

Figure 5.

Effect of current on collection efficiency in vivo for LE (red) and yaGfl (purple). The collection efficiency was calculated by dividing the moles per minute infused (measured by LC-MS^2) divided by the moles per minute collected at the MD probe (based on laboratory concentrations). The error bars represent the SEM for $n = 3$ replicates.

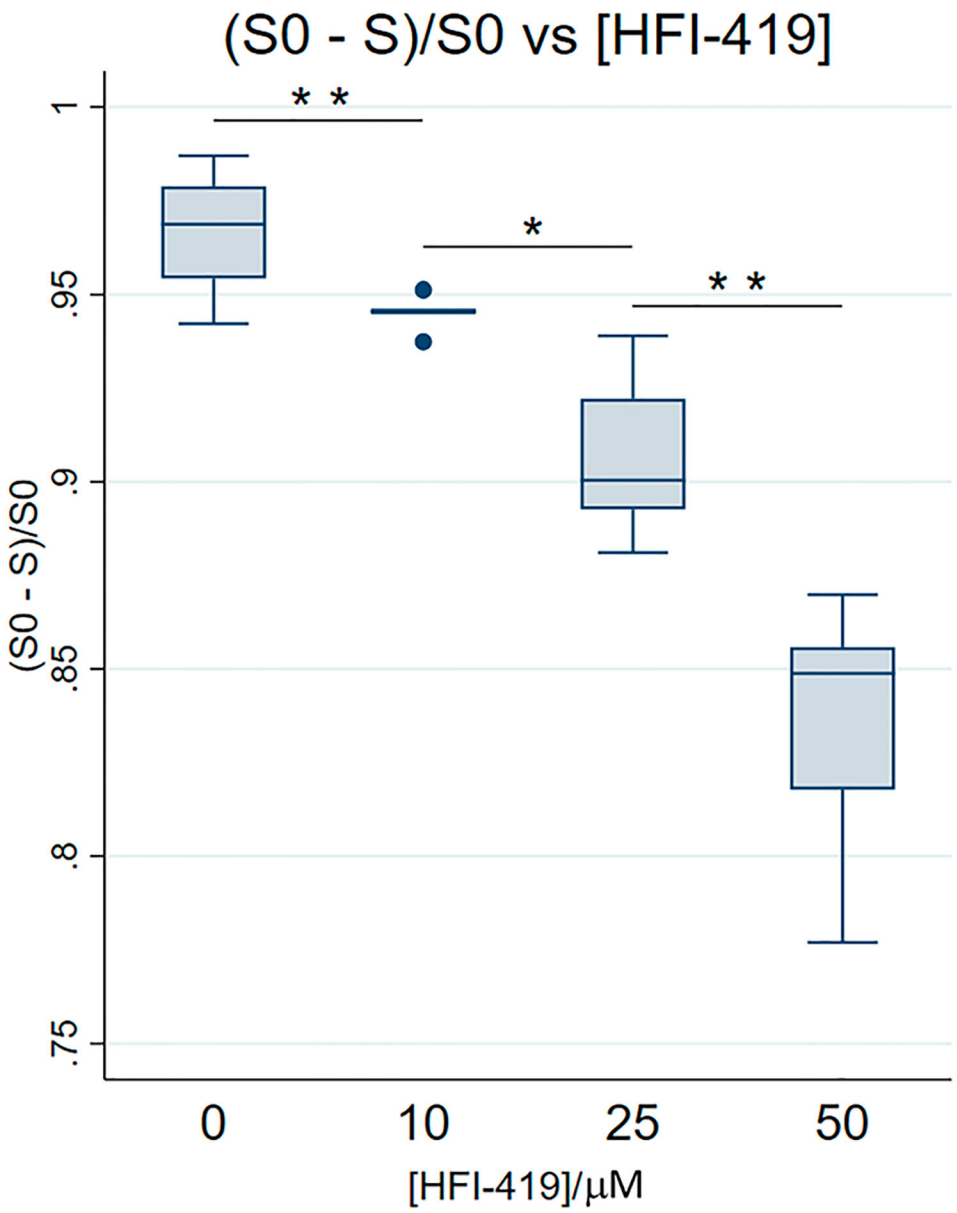

Figure 6.

Effect of HFI-419 concentration on product formation. Differences in means were determined using *t* test. The variances of the 25 mM and 10 mM data were unequal (*F*-test), so *t* testing was carried out with unequal variances. The other two tests were carried out with the assumption of equal variances based on their *F*-ratios. The single asterisk (*) indicates $p < 0.05$ and the double asterisk (**) indicates $p < 0.01$. The error bars indicate the SEM of $n = 15$ replicates for 0 μM inhibitor (5 replicates from each rat) and $n = 5$ replicates for the 10, 25, and 50 μM inhibitor concentrations.